Title

Molecular Characterization of Brown Carbon in Biomass Burning Aerosol Particles

Permalink

https://escholarship.org/uc/item/3mg289pj

Journal

Environmental Science and Technology, 50(21)

ISSN

0013-936X

Authors

Lin, Peng
Aiona, Paige K
Li, Ying
et al.

Publication Date

2016-11-01

DOI

10.1021/acs.est.6b03024

Peer reviewed

Molecular Characterization of Brown Carbon in Biomass Burning Aerosol Particles

Peng Lin,[†] Paige K. Aiona,[‡] Ying Li,[§,⊥] Manabu Shiraiwa,[‡,§] Julia Laskin,[∥] Sergey A. Nizkorodov,[‡] and Alexander Laskin[*,†]

[†]Environmental Molecular Sciences Laboratory, Pacific Northwest National Laboratory, Richland, Washington 99354, United States
[‡]Department of Chemistry, University of California, Irvine, California 92697, United States
[§]Multiphase Chemistry Department, Max Planck Institute for Chemistry, Mainz, 55128, Germany
[∥]Physical Sciences Division, Pacific Northwest National Laboratory, Richland, Washington 99354, United States
[⊥]National Institute for Environmental Studies, Tsukuba-City, Ibaraki 305-8506 Japan

ⓢ *Supporting Information*

ABSTRACT: Emissions from biomass burning are a significant source of brown carbon (BrC) in the atmosphere. In this study, we investigate the molecular composition of freshly emitted biomass burning organic aerosol (BBOA) samples collected during test burns of sawgrass, peat, ponderosa pine, and black spruce. We demonstrate that both the BrC absorption and the chemical composition of light-absorbing compounds depend significantly on the type of biomass fuels. Common BrC chromophores in the selected BBOA samples include nitro-aromatics, polycyclic aromatic hydrocarbon derivatives, and polyphenols spanning a wide range of molecular weights, structures, and light absorption properties. A number of biofuel-specific BrC chromophores are observed, indicating that some of them may be used as source-specific markers of BrC. On average, ∼50% of the light absorption in the solvent-extractable fraction of BBOA can be attributed to a limited number of strong BrC chromophores. The absorption coefficients of BBOA are affected by solar photolysis. Specifically, under typical atmospheric conditions, the 300 nm absorbance decays with a half-life of ∼16 h. A "molecular corridor" analysis of the BBOA volatility distribution suggests that many BrC compounds in the fresh BBOA have low saturation mass concentration (<1 μg m^{-3}) and will be retained in the particle phase under atmospherically relevant conditions.
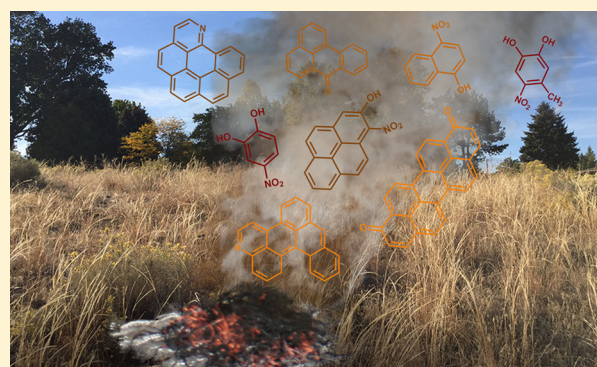
INTRODUCTION

Atmospheric brown carbon (BrC) is a common term for organic aerosol (OA) constituents that efficiently absorb solar and terrestrial radiation, and therefore have ultimate impact on climate forcing.[1−6] However, quantitative predictions of the contribution of BrC to the overall light absorption are still challenging because of the chemical complexity and source diversity of BrC.[7,8] BrC constituents are present both in primary aerosols emitted from combustion sources[9] and in secondary organic aerosols (SOA).[7] In some cases, the overall light-absorbing properties of SOA are determined by trace amounts of strong chromophores with highly specific molecular structures.[10] Additionally, light absorption properties of OA are influenced by intermolecular interactions resulting in formation of charge−transfer complexes between different OA molecules.[11,12] Numerous studies indicate that the optical properties of BrC evolve significantly as a result of various atmospheric processes such as oxidation,[13,14] solar irradiation,[15,16] changes in temperature[17] and relative humidity.[18−20] These factors make the chemical composition and concentration of BrC chromophores highly variable across sources and locations,[7,8] which in turn results in high uncertainties in predicting and mitigating their climate effects.[1,21,22]

Biomass burning organic aerosol (BBOA) has been identified as an important contributor to "primary BrC".[9,23−25] High columnar light absorbing levels have been observed in regions with high biomass burning activity.[26] A recent study reported that in the rural regions of the southeastern United States a majority of light absorption from BrC is associated with BBOA, with minor contributions from biogenic SOA.[27] Optical properties of BrC differ substantially among individual studies, with absorption Ångström exponent (AAE) values ranging from 1.5 to 12.[9,21,23,28] These differences are attributed to the compositional diversity of BrC originating from different sources. Furthermore, the optical properties of BrC may
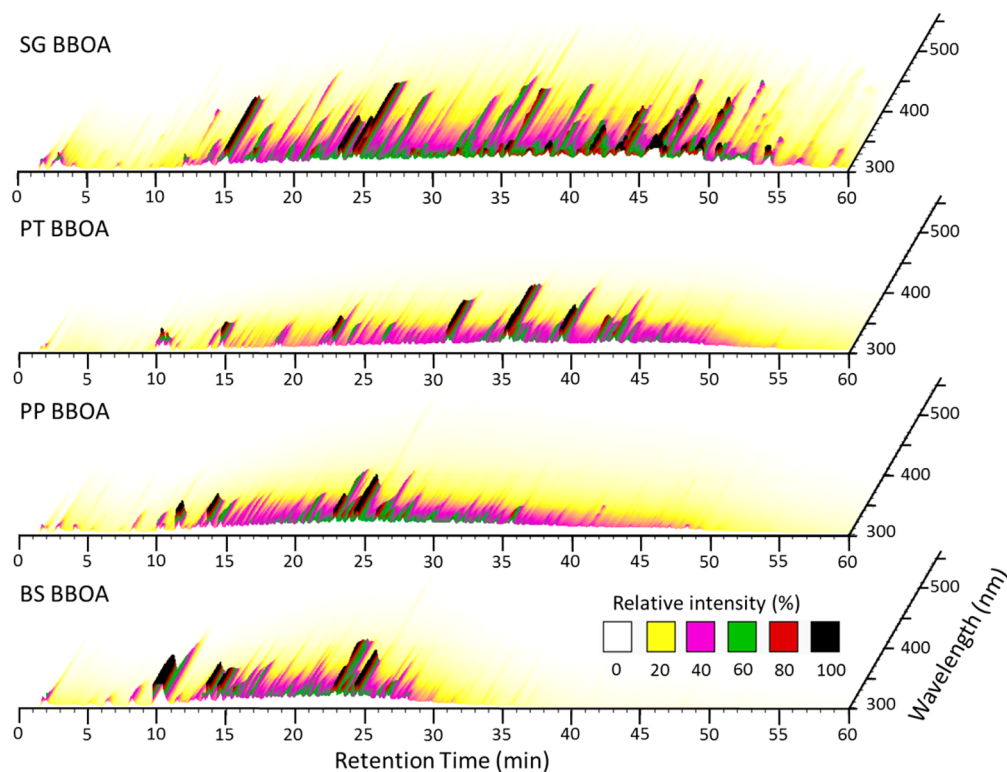
Figure 1. HPLC/PDA chromatograms of BBOA collected during burning of four biomass fuels: sawgrass (SG), peat (PT), ponderosa pine (PP), and black spruce (BS). The x-axis is retention time, the y-axis is the UV−vis absorption wavelength and color denotes the absorbance intensity recorded by the PDA detector.

change as BBOA ages in the atmosphere,[29−31] whereas the effect of aging on light absorption strongly depends on the molecular structures of BrC.[15,16,32] It follows that structural characterization of BrC chromophores will facilitate understanding of their photochemical stability and chemical transformations necessary for the accurate prediction of radiative forcing by BrC.[3]

The major challenge in the chemical characterization of BrC is distinguishing its light absorbing components (chromophores) from a majority of nonabsorbing aerosol constituents. The combination of high performance liquid chromatography (HPLC), photodiode array (PDA) spectrophotometry, and high resolution mass spectrometry (HRMS) is a powerful platform for the characterization of BrC chromophores. This technique has been previously used for characterization of BrC in laboratory-generated SOA[33,34] and in ambient aerosols and cloudwater impacted by the biomass burning.[35−38]

In this paper, we demonstrate the utility of the HPLC/PDA/HRMS platform for characterizing the molecular composition and optical properties of BrC chromophores present in a group of BBOA samples collected in a field study. We show that this approach can be used for the detailed analysis of the major BrC chromophores in the solvent-extractable fraction of BBOA, and assessment of their common versus source-specific appearance in BBOA. We also examine photodegradation of BrC chromophores by sunlight and the distribution of saturation mass concentrations of organic compounds in BBOA particles.

■ EXPERIMENTAL SECTION

Details about the experimental methods are described in Appendix I of SI. Briefly, BBOA samples were collected during the fourth Fire Lab at Missoula Experiment (FLAME-4).[39] We

focus on BrC emitted from burning of four biofuels: sawgrass (SG), peat (PT), ponderosa pine (PP), and black spruce (BS). These are representative biomass materials consumed by fires in grassland, peatland, and forest areas.[40,41] The FLAME-4 was designed to simulate fire emissions of "real-world" biomass burning activities.[39] Therefore, the combustion efficiencies of these biofuels were different and affected by many factors such as structure of the fuel assembly prior to ignition, moisture content and environmental variables.[42,43] Although the intent of this paper is to characterize BrC emitted from different biofuels, it should be noted that the chemical composition of BrC may also depend on the burning condition.

Particles were collected using a 10-stage Micro-Orifice Uniform Deposit Impactor (MOUDI, MSP, Inc.). Samples on the sixth and seventh impactor stages were combined together, extracted in 2 mL acetonitrile by ultrasonic extraction, and filtered with 0.45 μm PTFE membrane filters. The resulting solutions were concentrated under N_2 flow to a volume of ∼50 μL, then ∼200 μL of ultrapure water was added to make samples compatible with HPLC analysis.

Chemical analysis was performed with a HPLC/PDA/HRMS platform.[33,34] Details about the experimental setup, data acquisition, peak deconvolution,[44] formula assignment,[45] are described in SI. The aromatic index (AI) and double-bond equivalent (DBE) values were calculated according to Koch and Dittmar's work.[46,47] The data used for "molecular corridor" analysis[48,49] were obtained through direct infusion ESI-HRMS analysis of the samples.[45]

The stability of the BrC chromophores was investigated by exposing the solutions of BBOA samples in 50% (v) water/acetonitrile to filtered UV irradiation from a Xe-lamp and tracking the solution absorbance at 300 nm as a function of the

exposure time. The actinic flux from the lamp was measured with actinometry and converted into an effective actinic flux from the sun under representative atmospheric conditions, as described in Appendix II of the SI.

■ RESULTS AND DISCUSSION

Figure 1 displays the HPLC/PDA chromatograms of four BBOA samples. The resulting chromatograms are clearly different. SG BBOA sample contain a substantial fraction of BrC chromophores that absorb at longer wavelength range (>400 nm), while BrC chromophores in the other three samples absorb mainly in the 300−400 nm wavelength range. A significant fraction of BrC chromophores in SG BBOA are observed at much longer retention time (RT) than those in BS BBOA, where a majority of the chromophores elute within 30 min. BrC in the other two samples also show different elution profiles, with major fractions eluting between 20 and 50 min for PT BBOA and between 10 and 40 min for PP BBOA. These differences indicate that the chemical composition and optical properties of BrC chromophores are substantially different between these four samples.

The chemical composition of BBOA was investigated using the HPLC/HRMS data acquired in both positive (+) and negative (−) ESI modes.[50] Compounds were detected as either sodium adducts, $[M + Na]^+$, or protonated species, $[M + H]^+$, in (+)ESI, and as deprotonated species $[M-H]^-$ in (−)ESI. We report all detected compounds as neutral species, unless stated otherwise. Comparison of the total ion chromatograms (TICs) shown in Figure S1 indicates differences in the selectivity and sensitivity of the (+)ESI and (−)ESI modes toward specific BBOA compounds. For example, in PP BBOA (Figure S1), the (+)ESI TIC is dominated by compounds with low DBE, such as $C_8H_{18}O_3$ (DBE = 0), $C_{16}H_{32}O_4$ (DBE = 1) and other peaks labeled in gray. These species are unlikely to be BrC chromophores due to the lack of polyconjugated double bonds. In contrast, compounds with higher DBE values, such as $C_{12}H_8O_3$ (DBE = 9, AI = 0.67) and $C_{16}H_{12}O_6$ (DBE = 11, AI = 0.5) are abundant in the (−)ESI TIC. These peaks are potential BrC chromophores due to their high unsaturation, as evident by high DBE values. Compounds with high AI values are most likely aromatic. Koch and Dittmar[46,47] classified compounds with AI > 0.5 as aromatic, and compounds with AI ≥ 0.67 as condensed aromatic. Based on this classification, $C_{12}H_8O_3$ with an AI of 0.67 is a condensed-aromatic species. A similar trend is also observed in the TICs of BS BBOA (Figure S2), with low-DBE and high-DBE compounds observed predominantly in the (+)ESI and the (−)ESI mode, respectively. In PT BBOA, high-DBE and potentially aromatic compounds are observed in both (+)ESI and (−)ESI modes (Figure S3). The most complex TICs are observed for SG BBOA (Figure S4). In addition to the low-DBE aliphatic compounds (e.g., $C_8H_{18}O_3$ (DBE = 0), $C_{14}H_{29}ON$ (DBE = 1) and others), some high-DBE and possibly aromatic compounds are also observed in this sample in the (+)ESI mode, for example, $C_{13}H_8O$ (DBE = 10, AI = 0.75), $C_{16}H_{10}O$ (DBE = 12, AI = 0.73), and $C_{34}H_{35}O_5N$ (DBE = 18, AI = 0.45). Additional high-DBE compounds are observed in the (−)ESI mode, e.g., $C_6H_5O_4N$ (DBE = 5, AI = 0.5), $C_{16}H_9O_3N$ (DBE = 13, AI = 0.79), and others.

BrC chromophores have been distinguished by examining time periods of the HPLC/HRMS data corresponding to the PDA absorption peaks extending into the near-UV and visible wavelength ranges.[33,34,36] The third analytical dimension provided by the PDA detector is immensely useful for this

task, however, the HPLC/PDA/HRMS analysis can still be ambiguous because of the large number of compounds in BBOA samples. The HPLC/PDA/HRMS results for SG BBOA sample will be used as an illustrative example of the identification of potential BrC chromophores and of the analytical challenges associated with this process. UV−vis and mass spectra of species observed at two different RT in SG BBOA are shown in Figure S5. In ideal situations, which, unfortunately, are not common, only one chromophore is detected in a chromatographic peak. For example, the (−)ESI mass spectrum shown in Figure S5b is dominated by a single abundant ion $[C_6H_4O_4N]^-$ with DBE = 5, which is most likely a chromophore. Although three ions, $C_4H_{11}O_3^+$, $C_8H_{19}O_3^+$, and $C_8H_{18}O_3Na^+$, are observed in the (+)ESI mass spectrum (Figure S5c), these species correspond to saturated compounds with DBE = 0 that are not chromophores. The corresponding UV−vis spectrum of a chromophore at RT = 15.0 min is characterized by a single absorption maximum (λ_{max}) around 345 nm (Figure S5a) consistent with the presence of a single chromophore at this RT. The UV−vis spectrum of 4-nitrocatechol, $C_6H_5O_4N$, with λ_{max} at 345 nm and a shoulder at 309 nm[51] matches exactly the spectrum shown in Figure S5a. Thus, the BrC chromophore at RT = 15 min is most likely 4-nitrocatechol.[52] We note that more detailed structural characterization of BrC chromophores using, for example, tandem mass spectrometry and comparison with reference standards,[37] could be possible but is outside the scope of this study.

In other cases, despite the advantages offered by the chromatographic separation and multiple detectors employed in HPLC/PDA/HRMS, the UV−vis and MS spectra are fairly complex and cannot be unambiguously assigned to a single compound. Figure S5d shows a UV−vis spectrum detected at RT = 50.6 min with several absorption maxima above 300 nm. The corresponding (−)ESI mass spectrum shows a single most abundant peak, $C_{25}H_{36}O_2$ (DBE = 8, AI = 0.26) (Figure S5e), which is a good candidate of a chromophore. However, the (+)ESI mass spectrum shown in Figure S5f contains additional ions including plausible BrC chromophores and species that cannot contribute to the observed light absorption. To further narrow down the list of possible candidates, we use comparative analysis of the extracted ion chromatograms (EICs) to distinguish ions strongly correlated with the PDA chromatographic peaks. Details of the data analysis are illustrated in Figure S6 and have been described in our previous publications.[33,34] EICs of eight molecules are strongly correlated with the PDA signal (Figure S6). Four of them, $C_{18}H_{38}O_3$, $C_{18}H_{37}ON$, $C_{17}H_{35}ON$, and $C_{16}H_{30}O$, have low DBE values (<3), and therefore are not chromophores. The EIC of $C_{13}H_{18}O$ (DBE = 5, AI = 0.33) has a larger peak eluting at 17.8 min and a smaller one eluting at 50.6 min, suggesting at least two isomers for this ion. The latter may possibly be a fragment of a larger molecule eluting at 50.6 min. Finally, three species with high DBE that may have substantial network of conjugated double bonds for light absorption, $C_{22}H_{34}O_6N_2$ (DBE = 7, AI = 0), $C_{27}H_{39}O_2N$ (DBE = 9, AI = 0.27), and $C_{48}H_{66}O_4N_4$ (DBE = 18, AI = 0.30), coelute at RT = 50.6 min. Thus, the complex UV−vis spectrum shown in Figure S5d may be attributed to light absorption by multiple BrC chromophores. Furthermore, there is always a possibility that the UV−vis spectrum originates from a species that is not detectable by ESI in either (+) or (−) modes, such as an unsubstituted PAH. These findings emphasize the challenge of identifying BrC
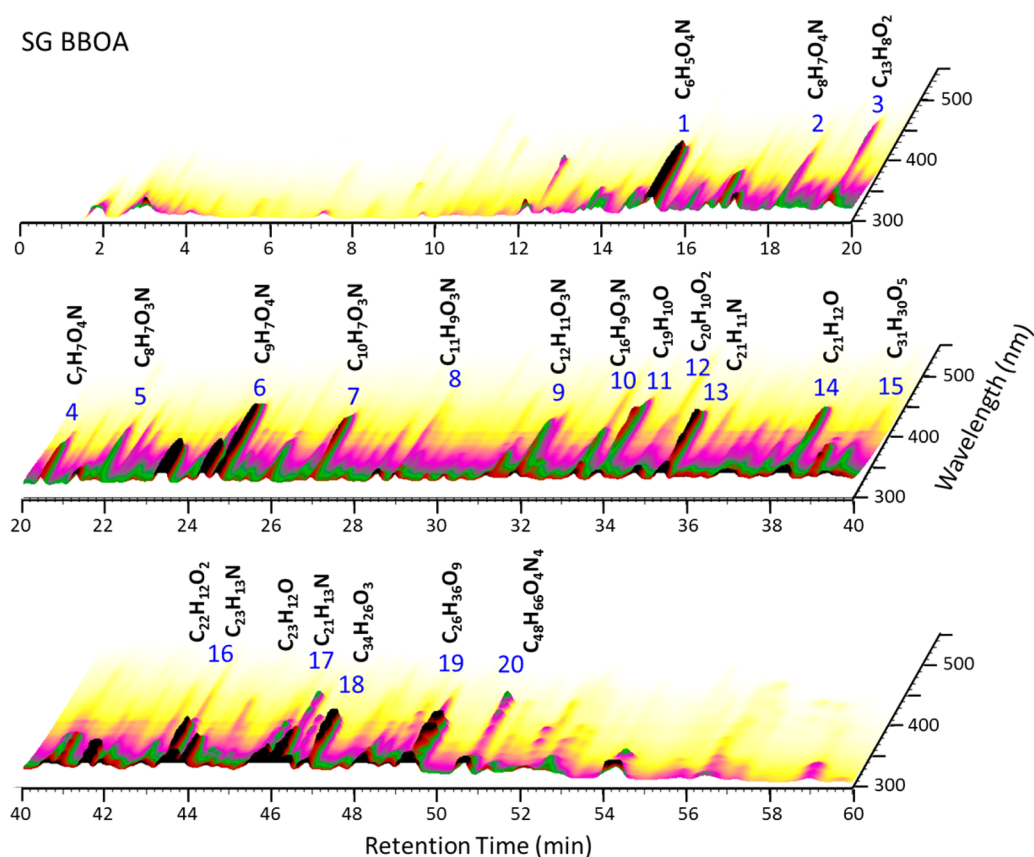
Figure 2. 3D-plot of HPLC/PDA chromatogram of BBOA from sawgrass (SG) burning. The peaks are labeled by the peak numbers and by the formulas of the most probable chromophores listed in Table S1.

chromophores in BBOA samples and suggest that acquisition of mass spectra in multiple ionization modes, along with the PDA spectra is essential for obtaining complementary information on the chemical composition of BrC.

Figure 2 shows the 3D-plot of HPLC/PDA results obtained for the SG BBOA sample along with formulas of the plausible chromophores, identified as described above. A full list of these compounds is summarized in Table S1, and the corresponding UV−vis spectra are shown in Figure S7. Our analysis suggests that BrC chromophores in SG BBOA are compounds with a wide range of molecular weights, structures, and optical properties. Chromophores eluting between 15 and 34 min are dominated by CHON compounds with zero or one N atom, O/N > 2 and AI > 0.5. These species are observed only in the (−)ESI mode indicating that they are likely nitrophenolic compounds. As mentioned earlier, $C_6H_5O_4N$ (RT = 15.0 min) has been identified as 4-nitrocatechol based on its UV−vis spectrum. $C_7H_7O_4N$ (RT = 20.4 min) has a very similar UV−vis spectrum (Figure S7a) to that of 4-nitrocatechol (Figures S7b and S5a). Therefore, considering the fact that substitution of a methyl group makes nearly no change to the UV−vis spectrum of nitro aromatic compounds, $C_7H_7O_4N$ is assigned as a methyl-substituted nitrocatechol.[34,36,53] Other chromophores including $C_8H_7O_4N$, $C_8H_7O_3N$, $C_9H_7O_4N$, and $C_{10}H_7O_4N$, have a UV−vis spectrum with a maximum at ∼380 nm and tailing absorption in the 400−450 nm range (Figure S7c-e), which is characteristic of nitro-phenolic compounds.[54] Their tentative structures proposed on the basis of literature data,[38,55,56] are shown in Figure S8a. These chromophores are mainly nitro-aromatic compounds with at

least one acidic functional group (e.g., hydroxyl- and carboxyl- substitution). Of particular interest is the $C_{16}H_9O_3N$ chromophore eluting at RT = 33.1 min, which may correspond to a 4-ring PAH with nitro- and hydroxyl- substitutions[38] (Figure S8a).

Nitro-phenols have been previously observed as the most abundant BrC chromophores in organic aerosols collected during the dry season of the Amazon rainforest,[35] and in cloudwater impacted by biomass burning in eastern China.[36] The latter study also demonstrated that these chromophores accounted for approximately half of measured light absorption. Similar nitro-phenolic compounds were observed in a suburban region of London during winter time, when domestic wood burning is the prevalent source of air pollutants.[57] A recent study quantified a group of nitrophenols in a total of 184 ambient aerosol samples collected in Hong Kong over 3 years and concluded that they were mainly associated with aged BBOA.[55] It has been proposed that methyl-nitrocatechols are formed by photooxidation of m-cresol emitted from wood combustion, and could be used as tracers for SOA formed by secondary photooxidation of primary biomass burning emissions.[58] During biomass burning, substituted phenols such as alkylphenols and methoxyphenols are produced from the pyrolysis of lignin,[59,60] which is the second most abundant component of plant material after cellulose.[61] These phenols are suggested to yield nitro-phenols through reactions with atmospheric radicals such as $^\bullet OH$, $^\bullet NO_2$, $^\bullet NO_3$, etc.[62] Our study of primary emitted BBOA samples suggests that nitro-phenols can also be produced during biomass burning, which is
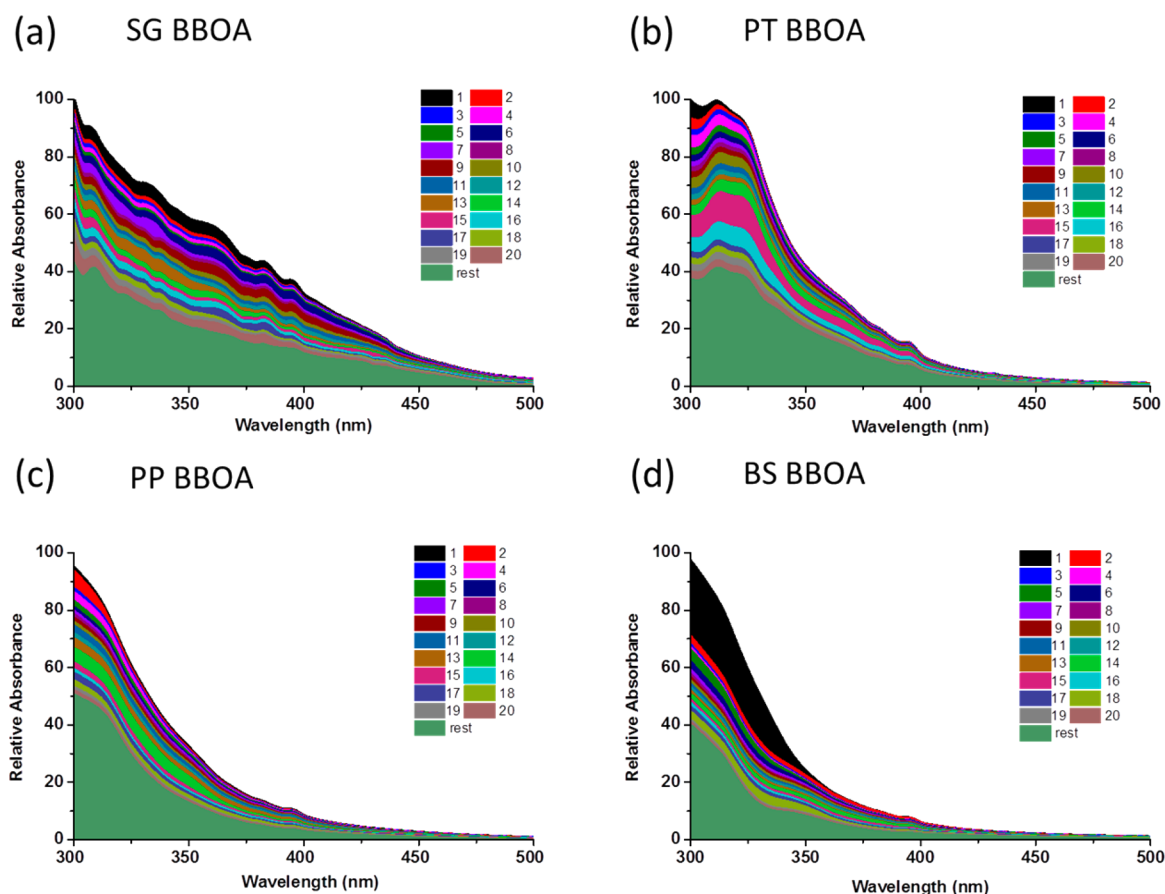
Figure 3. Relative contribution of the 20 most absorbing BrC chromophores detected in four BBOA samples collected from burning of (a) sawgrass (SG), (b) peat (PT), (c) ponderosa pine (PP), and (d) black spruce (BS) with respect to the total light absorption. The numbers for the color coding are the same denoting the 20 major PDA peaks on the HPLC/PDA chromatograms shown in Figure 2 and Figure S9−S11, respectively.

an oxidation process and releases a large amount of heat, NO_x, CO, and reactive volatile organic compounds (VOCs).[39,63]

A number of strong chromophores are observed as CHO compounds in the SG BBOA sample. They elute at RT ranging from 34 to 50 min and are detected more efficiently using (+)ESI. Their elemental formulas contain more than 17 carbons and 1−3 oxygens with AI > 0.67, indicating they are likely either oxygenated or O-heterocyclic PAHs (O-PAHs). Several reduced nitrogen compounds, such as $C_{21}H_{13}N$, $C_{21}H_{11}N$, and $C_{23}H_{13}N$, are also observed. Their high AI values suggest that they are N-heterocyclic PAHs (N-PAHs) with 4 to 6 aromatic rings fused together. Tentative molecular structures of these species are illustrated in Figure S8b,c. It has been reported that biomass burning produces substantial amounts of PAHs in both the gas- and particle-phase.[64] It is reasonable to assume that PAH derivatives such as O-PAHs and N-PAHs are also present in primary BBOA samples. The UV−vis spectra of PAHs with 4−6 rings typically contain multiple absorption peaks in the range of 300−400 nm.[65,66] In our study, the UV−vis spectra of PAH derivatives exhibit significant absorption at longer, 400−500 nm, wavelengths (e.g., Figure S7f−l). The observed red shift of the absorption band could be attributed to the fact that O and N atoms in O-PAHs and N-PAHs possess nonbonding electron lone pairs, which are responsible for the n-π* transitions in addition to the π−π* transitions originating from the PAH π-electron system.[67] Thus, the heterocyclic O-PAHs and N-PAHs may

absorb more solar radiation in the visible wavelength range than their corresponding PAHs.

The HPLC/PDA data and the BrC chromophore assignments obtained for the other three BBOA samples (PT, PP and BS) are shown in Figures S9−S11 and Table S1. Many strong and weak chromophores are observed in these samples, most of which are different from the chromophores identified in the SG BBOA sample. Although several nitro-aromatic compounds, such as $C_6H_5O_4N$ and $C_7H_7O_4N$, have been observed in all the samples, their relative contributions to the overall light absorption are not as significant in the PP, PT, and BS BBOA in comparison with SG BBOA. Instead, the chemical composition of the major chromophores in these three samples is dominated by CHO compounds with 7−28 carbons and 3−8 oxygens (Table S1), indicating their higher oxidation state than the chromophores detected in the SG BBOA sample. According to the structures of plant tissue material and the molecular markers of BBOA reported in the literature,[64] tentative molecular structures of these chromophores can be suggested (Figure S12). For example, based on the molecular formula and on the distinctive absorption spectrum,[68] $C_8H_8O_3$ likely corresponds to vanillin, a phenolic aldehyde produced from lignin pyrolysis.[60] $C_9H_6O_3$ and $C_{10}H_8O_4$ are probably derived from coumarin.[69] $C_{13}H_8O_5$ and $C_{13}H_8O_6$ may refer to compounds with hydroxyl substitutions derived from xanthone.[70,71] Compounds such as $C_{15}H_{10}O_6$, $C_{16}H_{12}O_6$, $C_{16}H_{12}O_7$, and $C_{17}H_{14}O_8$ may be polyphenols composed of flavone backbone and other oxygenated functional groups.[72]

Flavone backbone is the core structure of natural pigments and condensed tannins.[73] Condensed tannins are the most abundant polyphenols in nature, widely found in all families of plants.[74] Thus, thermal breakdown or pyrolysis of plant polyphenolic compounds such as lignin, lignans, and tannins during combustion[60,64] may be an important source of BrC chromophores in BBOA.

Comparison between the PT, PP, and BS BBOA samples reveals a variety of BrC chromophores common and unique for different BBOA. For clarity, Figure S13 shows the 10−40 min segments of HPLC/PDA density maps of PT, PP, and BS BBOA. Several distinct groups of chromophores are readily distinguished and their corresponding elemental formulas are listed. In the cases when several species can be assigned as BrC chromophores on the basis of the correlation between their EICs and the PDA peak, the elemental composition associated with the most abundant MS feature is chosen as the representative species (a full list of formulas is included in Table S1). Several common chromophores appear repeatedly in different samples. For instance, $C_8H_8O_3$, $C_9H_8O_3$, and $C_9H_7O_3N$ are observed in all three samples, but their relative contributions to the total light absorption are different. For example, $C_8H_8O_3$ at RT = 10.0 min corresponds to the most abundant PDA peak observed in the BS sample, whereas its contribution in the PP and PT samples is minor. In these two samples, very similar PDA absorption peaks and identical elemental formulas are detected during 12−28 min of RT. This similarity suggests the common nature of the PP and BS biomass fuel, as both of them are coniferous trees.

A significant fraction of light absorption in the PT sample is contributed by chromophores eluting after 30 min (Figure S13), implying they are more hydrophobic than the major chromophores in the PP and BS samples. The top three abundant PDA peaks in the PT sample correspond to compounds with formulas $C_{18}H_{16}O_6$, $C_{18}H_{16}O_5$, and $C_{19}H_{18}O_5$. These three compounds are absent in the other samples. Similarly, $C_{18}H_{16}O_4$ and $C_{20}H_{28}O_3$ are unique chromophores solely detected in the PP sample. These results suggest that the chemical composition of BrC chromophores and their relative abundance depend on the type of biomass fuel (and probably also on the burning conditions). Those source-specific chromophores may be used as molecular markers for BrC apportioned to specific types of biomass burning sources.

Understanding source-specific apportionment of BrC is useful in modeling its climate forcing effects on the basis of emission inventory. Overall, OA are composed of a myriad of organic compounds from a variety of sources, most of which do not absorb solar radiation in the visible range. A traditional molecular tracer of BBOA used for aerosol source apportionment is levoglucosan, which does not absorb visible and near-UV radiation. Since BrC chromophores appear to have different distributions in BBOA of different origin, the concentration of a single compound, such as levoglucosan, may not be correlated with overall light absorption by BrC. Thus, using levoglucosan as a tracer indicating the extent of the light absorption by BBOA may result in inherent uncertainties. The results of our study suggest that selected abundant chromophores within BrC mixtures may be potentially used as molecular markers to estimate total BrC light absorption of BBOA. Those BrC molecular tracers may be potentially used for more accurate emission inventories of BrC for atmospheric models.

It has been reported that ∼90% of BBOA can be extracted into moderately polar organic solvents, such as methanol or acetonitrile.[9,75] It would be worthwhile to evaluate the contributions of the identified strong chromophores to the overall UV−vis absorbance measured in the acetonitrile extracts of each of the BBOA samples (Figure 3). Figure 3a shows the overall UV−vis absorbance of the SG BBOA sample with relative contributions from the 20 most absorbing BrC chromophores labeled in Figure 2. Overall, ∼50% of the bulk BrC absorbance in the wavelength range of 300−500 nm may be attributed to these strong chromophores. Chromophores 1−10 are mainly nitro-phenols and their derivatives, which account for ∼25% of the overall light absorbance by SG BBOA. The PAH derivatives (BrC chromophores 11 to 20) account for another ∼25% fraction of the total absorption. The remaining ∼50% of the bulk absorption could be attributed to a myriad of weak chromophores with either lower concentration or smaller molar absorption coefficient, and charge transfer complexes formed between large molecules of BBOA.[11,12]

Similarly, as shown in Figures 3b−d, ∼ 40−60% of the overall light absorption in the extracts of PT, PP, and BS BBOA may be attributed to the 20 strong chromophores labeled in Figures S9−S11. On the basis of the HPLC/PDA data (Figures 1, 2 and Figures S9−S11) and the results shown in Figure 3, light absorption in the visible range (>400 nm) is mainly composed of the extended tails of the major BrC chromophores. Particularly, in the BS BBOA sample, $C_8H_8O_3$ chromophore accounts for ∼30% of light absorption at 300 nm and ∼10% at 350 nm. Since BrC chromophores in the PP, PT, and BS BBOA are mainly aromatic compounds with multiple hydroxyl and aldehyde/ketone groups, part of light absorption properties of these BBOA samples may originate from intermolecular interactions resulting in formation of charge-transfer complexes.[11,12] Moreover, aromatic compounds with multiple hydroxyl groups may form complexes with transition metals.[55,76,77] Such complexes may additionally enhance the light absorption properties of the organic ligands. Therefore, it is of particular interest to investigate the effects of transition metals on BrC absorption in future studies. Overall, numerous chromophores with varying concentrations and light absorption properties contribute to light absorption by BrC. The results in Figure 3 suggest that a considerable fraction of light absorption can be attributed to a limited number of strong chromophores. Although the exact molecular compositions of these chromophores are complex and diverse, some features on their core structures and functional groups are elucidated. These strong chromophores may serve as representative species for studying the reactivity of BrC under atmospheric aging processes.[16,17,30,31] Understanding the evolution of the optical properties of BrC and the underlying reaction mechanisms during atmospheric aging will benefit the evaluation of BrC's impacts on the direct radiative forcing of climate.[6]

The HPLC/PDA/HRMS analysis described above focuses on the composition and absorption spectra of *fresh* BBOA samples. However, the properties of BBOA may change as a result of chemical aging, for example, photobleaching, and physical aging, for example, selective evaporation of higher-volatility compounds primary particles. To assess the potential importance of these aging processes, we examined the stability of the light absorption by the BrC chromophores in the BBOA samples with respect to UV photobleaching. In general, the samples became less absorbing after the UV irradiation (Appendix II of SI). For example, Figure S15 shows that the
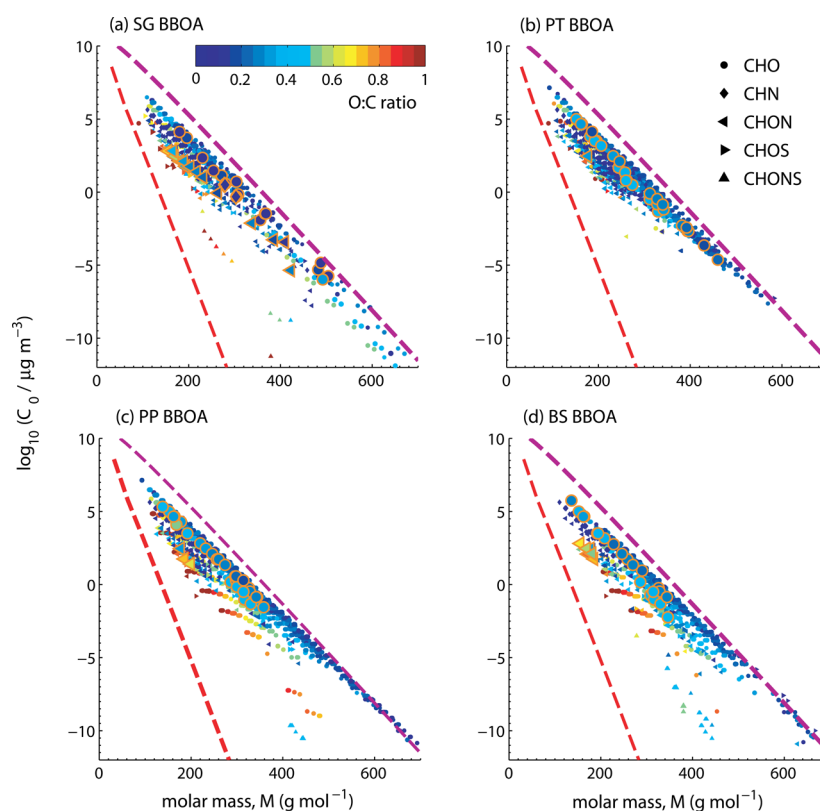
Figure 4. Molecular corridor of saturation mass concentration (C_0) vs molar mass (M) for BBOA samples collected from burning of (a) sawgrass (SG), (b) peat (PT), (c) ponderosa pine (PP), and (d) black spruce (BS), respectively. The dashed lines represent linear alkanes C_nH_{2n+2} (purple with O:C = 0) and sugar alcohols $C_nH_{2n+2}O_n$ (red with O:C = 1). The small markers represent individual compounds color-coded by O:C ratio. The size of the small markers is logarithmically scaled by the intensity of MS signal. The larger markers with orange edge indicate the 20 most absorbing BrC chromophores detected in these four BBOA samples, respectively.

absorption spectrum of PT BBOA decreases at all wavelengths after irradiation. The decrease in absorbance does not follow a single exponential decay because different chromophores decompose at different rates, as shown in Figure S16. However, on average, the absorbance decays with a half-life of 16.5 h under the conditions corresponding to 24-h average radiation flux in Los Angeles in summer. This relatively rapid evolution of the absorption characteristics may change the radiative forcing of BBOA after photochemical aging.

Fresh smoke particles commonly lose mass through evaporation.[78] If chromophores are much less or much more volatile than nonabsorbing BBOA compounds, evaporation may alter the absorption properties of BBOA. To examine this effect, we estimated the pure compound saturation mass concentration (C_0) distribution of the four BBOA samples based on the "molecular corridor" approach, which relies on an empirically observed inverse correlation between C_0 and molar mass of OA compounds.[48,49] Figure 4 shows the result of this estimation. The observed compounds (color-coded by atomic O:C ratio) fall into the space with upper and lower limiting boundaries represented by linear alkanes (C_nH_{2n+2}, O:C = 0; purple dashed line) and sugar alcohols ($C_nH_{2n+2}O_n$, O:C = 1; red dashed line), respectively. All of the four BBOA samples cover a wide range of C_0 from 10^{-10} $\mu g \ m^{-3}$, characteristic of extremely low volatility organic compounds, to 10^7 $\mu g \ m^{-3}$, characteristic of highly volatile compounds that should readily evaporate from particles. (Under typical ambient conditions, compounds with C_0 above 1 $\mu g \ m^{-3}$ are more likely to be found in the gas-phase.[79,80]) Most observed compounds have low

O:C ratio and thus are located closer to the alkane line. Some highly oxidized and low volatility compounds from SG, PP, and BS are found in the lower middle space of the molecular corridor, while those are not observed in the PT sample. The most abundant BrC chromophores discussed earlier are shown with larger symbols in Figure 4. In SG and PT BBOA, BrC chromophores have a wide volatility range, and at least some of them are expected to evaporate from the particles. This implies that physical aging by evaporation may have a rather significant effect on the optical properties of BBOA.

■ ASSOCIATED CONTENT

Ⓢ Supporting Information

The Supporting Information is available free of charge on the ACS Publications website at DOI: 10.1021/acs.est.6b03024.

Additional description of experimental procedures and results: Appendix I provide details of the experimental section; Table S1 lists elemental formulas of BrC chromophores found in the four BBOA samples; Figures S1−S4 show the LC/MS chromatograms of the four analyzed BBOA samples; Figure S5 shows examples of PDA and MS results obtained for selected chromophores; Figure S6 shows an example demonstrating the method used for identification of major BrC chromophores; Figure S7 shows UV−vis spectra of the strong chromophores observed in sawgrass (SG) BBOA; Figure S8 and S12 show the tentative molecular structures of BrC chromophores; Figures S9−S11 show the HPLC/ PDA chromatogram of BBOA from peat (PT), ponder-

osa pine (PP), and black spruce (BS) burning, respectively; Figure S13 shows the common and source specific BrC chromophores from different BBOA samples; Appendix II and Figures S14−S17 describe the method and results for the BrC photostability test (PDF)

■ **AUTHOR INFORMATION**

Corresponding Author

*Phone: +1 509 371-6129; e-mail: alexander.laskin@pnnl.gov.

Notes

The authors declare no competing financial interest.

■ **ACKNOWLEDGMENTS**

■ **REFERENCES**

(1) Bahadur, R.; Praveen, P. S.; Xu, Y. Y.; Ramanathan, V. Solar absorption by elemental and brown carbon determined from spectral observations. *Proc. Natl. Acad. Sci. U. S. A.* **2012**, *109* (43), 17366−17371.

(2) Chung, C. E.; Ramanathan, V.; Decremer, D. Observationally constrained estimates of carbonaceous aerosol radiative forcing. *Proc. Natl. Acad. Sci. U. S. A.* **2012**, *109* (29), 11624−11629.

(3) Feng, Y.; Ramanathan, V.; Kotamarthi, V. R. Brown carbon: A significant atmospheric absorber of solar radiation? *Atmos. Chem. Phys.* **2013**, *13* (17), 8607−8621.

(4) Lin, G. X.; Penner, J. E.; Flanner, M. G.; Sillman, S.; Xu, L.; Zhou, C. Radiative forcing of organic aerosol in the atmosphere and on snow: Effects of SOA and brown carbon. *J. Geophys Res-Atmos* **2014**, *119* (12), 7453−7476.

(5) Ramanathan, V.; Li, F.; Ramana, M. V.; Praveen, P. S.; Kim, D.; Corrigan, C. E.; Nguyen, H.; Stone, E. A.; Schauer, J. J.; Carmichael, G. R.; Adhikary, B.; Yoon, S. C. Atmospheric brown clouds: Hemispherical and regional variations in long-range transport, absorption, and radiative forcing. *J. Geophys. Res.* **2007**, *112* (D22), D22S21.

(6) Ramanathan, V.; Ramana, M. V.; Roberts, G.; Kim, D.; Corrigan, C.; Chung, C.; Winker, D. Warming trends in Asia amplified by brown cloud solar absorption. *Nature* **2007**, *448* (7153), 575−578.

(7) Moise, T.; Flores, J. M.; Rudich, Y. Oprtical properties of secondary organic aerosols and their changes by chemical processes. *Chem. Rev.* **2015**, *115* (10), 4400−4439.

(8) Laskin, A.; Laskin, J.; Nizkorodov, S. A. Chemistry of atmospheric brown carbon. *Chem. Rev.* **2015**, *115* (10), 4335−4382.

(9) Chen, Y.; Bond, T. C. Light absorption by organic carbon from wood combustion. *Atmos. Chem. Phys.* **2010**, *10* (4), 1773−1787.

(10) Laskin, J.; Laskin, A.; Nizkorodov, S. A.; Roach, P.; Eckert, P.; Gilles, M. K.; Wang, B. B.; Lee, H. J.; Hu, Q. C. Molecular selectivity of brown carbon chromophores. *Environ. Sci. Technol.* **2014**, *48* (20), 12047−12055.

(11) Phillips, S. M.; Smith, G. D. Light absorption by charge transfer complexes in brown carbon aerosols. *Environ. Sci. Technol. Lett.* **2014**, *1* (10), 382−386.

(12) Phillips, S. M.; Smith, G. D. Further evidence for charge transfer complexes in brown carbon aerosols from excitation-emission matrix fluorescence spectroscopy. *J. Phys. Chem. A* **2015**, *119* (19), 4545−4551.

(13) Lambe, A. T.; Cappa, C. D.; Massoli, P.; Onasch, T. B.; Forestieri, S. D.; Martin, A. T.; Cummings, M. J.; Croasdale, D. R.; Brune, W. H.; Worsnop, D. R.; Davidovits, P. Relationship between oxidation level and optical properties of secondary organic aerosol. *Environ. Sci. Technol.* **2013**, *47* (12), 6349−6357.

(14) Sareen, N.; Moussa, S. G.; McNeill, V. F. Photochemical aging of light-absorbing secondary organic aerosol material. *J. Phys. Chem. A* **2013**, *117* (14), 2987−2996.

(15) Lee, H. J.; Aiona, P. K.; Laskin, A.; Laskin, J.; Nizkorodov, S. A. Effect of solar radiation on the optical properties and molecular composition of laboratory proxies of atmospheric brown carbon. *Environ. Sci. Technol.* **2014**, *48* (17), 10217−10226.

(16) Zhao, R.; Lee, A. K. Y.; Huang, L.; Li, X.; Yang, F.; Abbatt, J. P. D. Photochemical processing of aqueous atmospheric brown carbon. *Atmos. Chem. Phys.* **2015**, *15* (11), 6087−6100.

(17) Rincon, A. G.; Guzman, M. I.; Hoffmann, M. R.; Colussi, A. J. Thermochromism of model organic aerosol matter. *J. Phys. Chem. Lett.* **2010**, *1* (1), 368−373.

(18) De Haan, D. O.; Hawkins, L. N.; Kononenko, J. A.; Turley, J. J.; Corrigan, A. L.; Tolbert, M. A.; Jimenez, J. L. Formation of nitrogen-containing oligomers by methylglyoxal and amines in simulated evaporating cloud droplets. *Environ. Sci. Technol.* **2011**, *45* (3), 984−991.

(19) Lee, A. K. Y.; Zhao, R.; Li, R.; Liggio, J.; Li, S. M.; Abbatt, J. P. D. Formation of light absorbing organo-nitrogen species from evaporation of droplets containing glyoxal and ammonium sulfate. *Environ. Sci. Technol.* **2013**, *47* (22), 12819−12826.

(20) Nguyen, T. B.; Lee, P. B.; Updyke, K. M.; Bones, D. L.; Laskin, J.; Laskin, A.; Nizkorodov, S. A. Formation of nitrogen- and sulfur-containing light-absorbing compounds accelerated by evaporation of water from secondary organic aerosols. *J. Geophys Res., Atmos.* **2012**, *117* (D1), n/a.

(21) Alexander, D. T. L.; Crozier, P. A.; Anderson, J. R. Brown carbon spheres in East Asian outflow and their optical properties. *Science* **2008**, *321* (5890), 833−836.

(22) Bond, T. C.; Bergstrom, R. W. Light absorption by carbonaceous particles: An investigative review. *Aerosol Sci. Technol.* **2006**, *40* (1), 27−67.

(23) Chakrabarty, R. K.; Moosmuller, H.; Chen, L. W. A.; Lewis, K.; Arnott, W. P.; Mazzoleni, C.; Dubey, M. K.; Wold, C. E.; Hao, W. M.; Kreidenweis, S. M. Brown carbon in tar balls from smoldering biomass combustion. *Atmos. Chem. Phys.* **2010**, *10* (13), 6363−6370.

(24) Lack, D. A.; Langridge, J. M.; Bahreini, R.; Cappa, C. D.; Middlebrook, A. M.; Schwarz, J. P. Brown carbon and internal mixing in biomass burning particles. *Proc. Natl. Acad. Sci. U. S. A.* **2012**, *109* (37), 14802−14807.

(25) Lukacs, H.; Gelencser, A.; Hammer, S.; Puxbaum, H.; Pio, C.; Legrand, M.; Kasper-Giebl, A.; Handler, M.; Limbeck, A.; Simpson, D.; Preunkert, S. Seasonal trends and possible sources of brown carbon based on 2-year aerosol measurements at six sites in Europe. *J. Geophys. Res.* **2007**, *112* (D23), D23S18.

(26) Arola, A.; Schuster, G.; Myhre, G.; Kazadzis, S.; Dey, S.; Tripathi, S. N. Inferring absorbing organic carbon content from AERONET data. *Atmos. Chem. Phys.* **2011**, *11* (1), 215−225.

(27) Washenfelder, R. A.; Attwood, A. R.; Brock, C. A.; Guo, H.; Xu, L.; Weber, R. J.; Ng, N. L.; Allen, H. M.; Ayres, B. R.; Baumann, K.; Cohen, R. C.; Draper, D. C.; Duffey, K. C.; Edgerton, E.; Fry, J. L.; Hu, W. W.; Jimenez, J. L.; Palm, B. B.; Romer, P.; Stone, E. A.; Wooldridge, P. J.; Brown, S. S. Biomass burning dominates brown carbon absorption in the rural southeastern United States. *Geophys. Res. Lett.* **2015**, *42* (2), 653−664.

(28) Lewis, K.; Arnott, W. P.; Moosmuller, H.; Wold, C. E. Strong spectral variation of biomass smoke light absorption and single scattering albedo observed with a novel dual-wavelength photoacoustic instrument. *J. Geophys. Res.* **2008**, *113* (D16), D16203.

(29) Adler, G.; Flores, J. M.; Abo Riziq, A.; Borrmann, S.; Rudich, Y. Chemical, physical, and optical evolution of biomass burning aerosols: a case study. *Atmos. Chem. Phys.* **2011**, *11* (4), 1491−1503.

(30) Forrister, H.; Liu, J.; Scheuer, E.; Dibb, J.; Ziemba, L.; Thornhill, K. L.; Anderson, B.; Diskin, G.; Perring, A. E.; Schwarz, J. P.; Campuzano-Jost, P.; Day, D. A.; Palm, B. B.; Jimenez, J. L.; Nenes, A.; Weber, R. J. Evolution of brown carbon in wildfire plumes. *Geophys. Res. Lett.* **2015**, *42* (11), 4623−4630.

(31) Zhong, M.; Jang, M. Dynamic light absorption of biomass-burning organic carbon photochemically aged under natural sunlight. *Atmos. Chem. Phys.* **2014**, *14* (3), 1517−1525.

(32) Amarnath, V.; Valentine, W. M.; Amarnath, K.; Eng, M. A.; Graham, D. G. The mechanism of nucleophilic-substitution of alkylpyrroles in the presence of oxygen. *Chem. Res. Toxicol.* **1994**, *7* (1), 56−61.

(33) Lin, P.; Laskin, J.; Nizkorodov, S. A.; Laskin, A. Revealing brown carbon chromophores produced in reactions of methylglyoxal with ammonium sulfate. *Environ. Sci. Technol.* **2015**, *49* (24), 14257−14266.

(34) Lin, P.; Liu, J. M.; Shilling, J. E.; Kathmann, S. M.; Laskin, J.; Laskin, A. Molecular characterization of brown carbon (BrC) chromophores in secondary organic aerosol generated from photo-oxidation of toluene. *Phys. Chem. Chem. Phys.* **2015**, *17* (36), 23312−23325.

(35) Claeys, M.; Vermeylen, R.; Yasmeen, F.; Gomez-Gonzalez, Y.; Chi, X. G.; Maenhaut, W.; Meszaros, T.; Salma, I. Chemical characterisation of humic-like substances from urban, rural and tropical biomass burning environments using liquid chromatography with UV/vis photodiode array detection and electrospray ionisation mass spectrometry. *Environ. Chem.* **2012**, *9* (3), 273−284.

(36) Desyaterik, Y.; Sun, Y.; Shen, X. H.; Lee, T. Y.; Wang, X. F.; Wang, T.; Collett, J. L. Speciation of ″brown″ carbon in cloud water impacted by agricultural biomass burning in eastern China. *J. Geophys Res-Atmos* **2013**, *118* (13), 7389−7399.

(37) Kitanovski, Z.; Grgic, I.; Yasmeen, F.; Claeys, M.; Cusak, A. Development of a liquid chromatographic method based on ultraviolet-visible and electrospray ionization mass spectrometric detection for the identification of nitrocatechols and related tracers in biomass burning atmospheric organic aerosol. *Rapid Commun. Mass Spectrom.* **2012**, *26* (7), 793−804.

(38) Zhang, X. L.; Lin, Y. H.; Surratt, J. D.; Weber, R. J. Sources, composition and absorption angstrom exponent of light-absorbing organic components in aerosol extracts from the Los Angeles Basin. *Environ. Sci. Technol.* **2013**, *47* (8), 3685−3693.

(39) Stockwell, C. E.; Yokelson, R. J.; Kreidenweis, S. M.; Robinson, A. L.; DeMott, P. J.; Sullivan, R. C.; Reardon, J.; Ryan, K. C.; Griffith, D. W. T.; Stevens, L. Trace gas emissions from combustion of peat, crop residue, domestic biofuels, grasses, and other fuels: configuration and Fourier transform infrared (FTIR) component of the fourth Fire Lab at Missoula Experiment (FLAME-4). *Atmos. Chem. Phys.* **2014**, *14* (18), 9727−9754.

(40) Stockwell, C. E.; Veres, P. R.; Williams, J.; Yokelson, R. J. Characterization of biomass burning emissions from cooking fires, peat, crop residue, and other fuels with high-resolution proton-transfer-reaction time-of-flight mass spectrometry. *Atmos. Chem. Phys.* **2015**, *15* (2), 845−865.

(41) van der Werf, G. R.; Randerson, J. T.; Giglio, L.; Collatz, G. J.; Mu, M.; Kasibhatla, P. S.; Morton, D. C.; DeFries, R. S.; Jin, Y.; van Leeuwen, T. T. Global fire emissions and the contribution of deforestation, savanna, forest, agricultural, and peat fires (1997−2009). *Atmos. Chem. Phys.* **2010**, *10* (23), 11707−11735.

(42) Bertschi, I.; Yokelson, R. J.; Ward, D. E.; Babbitt, R. E.; Susott, R. A.; Goode, J. G.; Hao, W. M. Trace gas and particle emissions from fires in large diameter and belowground biomass fuels. *J. Geophys Res-Atmos* **2003**, *108* (D13), 8472.

(43) Yokelson, R. J.; Burling, I. R.; Urbanski, S. P.; Atlas, E. L.; Adachi, K.; Buseck, P. R.; Wiedinmyer, C.; Akagi, S. K.; Toohey, D. W.; Wold, C. E. Trace gas and particle emissions from open biomass burning in Mexico. *Atmos. Chem. Phys.* **2011**, *11* (14), 6787−6808.

(44) Pluskal, T.; Castillo, S.; Villar-Briones, A.; Oresic, M. MZmine 2: Modular framework for processing, visualizing, and analyzing mass spectrometry-based molecular profile data. *BMC Bioinf.* **2010**, *11*, 395−405.

(45) Roach, P. J.; Laskin, J.; Laskin, A. Higher-order mass defect analysis for mass spectra of complex organic mixtures. *Anal. Chem.* **2011**, *83* (12), 4924−4929.

(46) Koch, B. P.; Dittmar, T. From mass to structure: an aromaticity index for high-resolution mass data of natural organic matter. *Rapid Commun. Mass Spectrom.* **2006**, *20* (5), 926−932.

(47) Koch, B. P.; Dittmar, T. From mass to structure: an aromaticity index for high-resolution mass data of natural organic matter (vol 20, pg 926, 2006). *Rapid Commun. Mass Spectrom.* **2016**, *30* (1), 250−250.

(48) Li, Y.; Pöschl, U.; Shiraiwa, M. Molecular corridors and parameterizations of volatility in the chemical evolution of organic aerosols. *Atmos. Chem. Phys.* **2016**, *16* (5), 3327−3344.

(49) Shiraiwa, M.; Berkemeier, T.; Schilling-Fahnestock, K. A.; Seinfeld, J. H.; Poschl, U. Molecular corridors and kinetic regimes in the multiphase chemical evolution of secondary organic aerosol. *Atmos. Chem. Phys.* **2014**, *14* (16), 8323−8341.

(50) Lin, P.; Rincon, A. G.; Kalberer, M.; Yu, J. Z. Elemental composition of HULIS in the Pearl River Delta region, China: Results inferred from positive and negative electrospray high resolution mass spectrometric data. *Environ. Sci. Technol.* **2012**, *46* (14), 7454−7462.

(51) Cornard, J. P.; Rasmiwetti; Merlin, J. C. , Molecular structure and spectroscopic properties of 4-nitrocatechol at different pH: UV-visible, Raman, DFT and TD-DFT calculations. *Chem. Phys.* **2005**, *309* (2−3), 239−249.

(52) Kahnt, A.; Behrouzi, S.; Vermeylen, R.; Safi Shalamzari, M.; Vercauteren, J.; Roekens, E.; Claeys, M.; Maenhaut, W. One-year study of nitro-organic compounds and their relation to wood burning in PM10 aerosol from a rural site in Belgium. *Atmos. Environ.* **2013**, *81*, 561−568.

(53) Perkampus, H.-H. *UV-Vis Atlas of Organic Compounds*; Weinheim: New York, 1992.

(54) Jacobson, M. Z. Isolating nitrated and aromatic aerosols and nitrated aromatic gases as sources of ultraviolet light absorption. *J. Geophys Res-Atmos* **1999**, *104* (D3), 3527−3542.

(55) Chow, K. S.; Huang, X. H. H.; Yu, J. Z. Quantification of nitroaromatic compounds in atmospheric fine particulate matter in Hong Kong over 3 years: field measurement evidence for secondary formation derived from biomass burning emissions. *Environmental Chemistry* **2016**, *13* (4), 665−673.

(56) Yee, L. D.; Kautzman, K. E.; Loza, C. L.; Schilling, K. A.; Coggon, M. M.; Chhabra, P. S.; Chan, M. N.; Chan, A. W. H.; Hersey, S. P.; Crounse, J. D.; Wennberg, P. O.; Flagan, R. C.; Seinfeld, J. H. Secondary organic aerosol formation from biomass burning inter-mediates: phenol and methoxyphenols. *Atmos. Chem. Phys.* **2013**, *13* (16), 8019−8043.

(57) Mohr, C.; Lopez-Hilfiker, F. D.; Zotter, P.; Prevot, A. S. H.; Xu, L.; Ng, N. L.; Herndon, S. C.; Williams, L. R.; Franklin, J. P.; Zahniser, M. S.; Worsnop, D. R.; Knighton, W. B.; Aiken, A. C.; Gorkowski, K. J.; Dubey, M. K.; Allan, J. D.; Thornton, J. A. Contribution of nitrated phenols to wood burning brown carbon light absorption in Detling, United Kingdom during winter time. *Environ. Sci. Technol.* **2013**, *47* (12), 6316−6324.

(58) Iinuma, Y.; Boge, O.; Grafe, R.; Herrmann, H. Methyl-nitrocatechols: Atmospheric tracer compounds for biomass burning secondary organic aerosols. *Environ. Sci. Technol.* **2010**, *44* (22), 8453−8459.

(59) Mazzoleni, L. R.; Zielinska, B.; Moosmuller, H. Emissions of levoglucosan, methoxy phenols, and organic acids from prescribed burns, laboratory combustion of wildland fuels, and residential wood combustion. *Environ. Sci. Technol.* **2007**, *41* (7), 2115−2122.

(60) Simoneit, B. R. T.; Rogge, W. F.; Mazurek, M. A.; Standley, L. J.; Hildemann, L. M.; Cass, G. R. Lignin pyrolysis products, lignans, and resin acids as specific tracers of plant classes in emissions from biomass combustion. *Environ. Sci. Technol.* **1993**, *27* (12), 2533−2541.

(61) Boerjan, W.; Ralph, J.; Baucher, M. Lignin biosynthesis. *Annu. Rev. Plant Biol.* **2003**, *54*, 519−546.

(62) Harrison, M. A. J.; Barra, S.; Borghesi, D.; Vione, D.; Arsene, C.; Iulian Olariu, R. Nitrated phenols in the atmosphere: a review. *Atmos. Environ.* **2005**, *39* (2), 231−248.

(63) Hatch, L. E.; Luo, W.; Pankow, J. F.; Yokelson, R. J.; Stockwell, C. E.; Barsanti, K. C. Identification and quantification of gaseous organic compounds emitted from biomass burning using two-dimensional gas chromatography-time-of-flight mass spectrometry. *Atmos. Chem. Phys.* **2015**, *15* (4), 1865−1899.

(64) Simoneit, B. R. T. Biomass burning - A review of organic tracers for smoke from incomplete combustion. *Appl. Geochem.* **2002**, *17* (3), 129−162.

(65) Bagley, S. P.; Wornat, M. J. Identification of five- to seven-ring polycyclic aromatic hydrocarbons from the supercritical pyrolysis of n-decane. *Energy Fuels* **2011**, *25* (10), 4517−4527.

(66) Talrose, V.; Stern, E. B.; Goncharova, A.A.; Messineva, N.A.; Trusova, N.V.; Efimkina, M.V. UV/Visible Spectra. In *NIST Chemistry WebBook, NIST Standard Reference Database Number 69*; Linstrom, P.J., Mallard, W.G., Eds.; National Institute of Standards and Technology: Gaithersburg MD, 20899, http://webbook.nist.gov, (retrieved March 31, 2016).

(67) Jonathan, Clayden; Nick, Greeves; Warren, a. S. *Organic Chemistry*. Oxford Press: 2012; p 1392.

(68) Robinson, R. A.; Kiang, A. K. The ionization constants of vanillin and two of its isomers. *Trans. Faraday Soc.* **1955**, *51*, 1398−1402.

(69) Fine, P. M.; Cass, G. R.; Simoneit, B. R. T. Chemical characterization of fine particle emissions from the wood stove combustion of prevalent United States tree species. *Environ. Eng. Sci.* **2004**, *21* (6), 705−721.

(70) Bruns, E. A.; Krapf, M.; Orasche, J.; Huang, Y.; Zimmermann, R.; Drinovec, L.; Mocnik, G.; El-Haddad, I.; Slowik, J. G.; Dommen, J.; Baltensperger, U.; Prevot, A. S. H. Characterization of primary and secondary wood combustion products generated under different burner loads. *Atmos. Chem. Phys.* **2015**, *15* (5), 2825−2841.

(71) Herring, C. L.; Faiola, C. L.; Massoli, P.; Sueper, D.; Erickson, M. H.; McDonald, J. D.; Simpson, C. D.; Yost, M. G.; Jobson, B. T.; VanReken, T. M. New methodology for quantifying polycyclic aromatic hydrocarbons (PAHs) using high-resolution aerosol mass spectrometry. *Aerosol Sci. Technol.* **2015**, *49* (11), 1131−1148.

(72) Quideau, S.; Deffieux, D.; Douat-Casassus, C.; Pouysegu, L. Plant polyphenols: chemical properties, biological activities, and synthesis. *Angew. Chem., Int. Ed.* **2011**, *50* (3), 586−621.

(73) Cammack, R.; Atwood, T.; Campbell, P.; Parish, H.; Smith, A.; Vella, F.; Stirling, J. *Oxford Dictionary of Biochemistry and Molecular Biology*; Oxford University Press: Oxford, 2006.

(74) J, P. L., Condensed tannins. In *Natural Products of Woody Plants I*; W, R. J., Ed.; Springer-Verlag: Berlin, Germany, 1989; pp 651−690.

(75) Cheng, Y.; He, K.-b.; Du, Z.-y.; Engling, G.; Liu, J.-m.; Ma, Y.-l.; Zheng, M.; Weber, R. J. The characteristics of brown carbon aerosol during winter in Beijing. *Atmos. Environ.* **2016**, *127*, 355−364.

(76) Deguillaume, L.; Leriche, M.; Desboeufs, K.; Mailhot, G.; George, C.; Chaumerliac, N. Transition metals in atmospheric liquid phases: Sources, reactivity, and sensitive parameters. *Chem. Rev.* **2005**, *105* (9), 3388−3431.

(77) Kitanovski, Z.; Grgic, I.; Vermeylen, R.; Claeys, M.; Maenhaut, W. Liquid chromatography tandem mass spectrometry method for characterization of monoaromatic nitro-compounds in atmospheric particulate matter. *J. Chromatogr. A* **2012**, *1268*, 35−43.

(78) May, A. A.; Lee, T.; McMeeking, G. R.; Akagi, S.; Sullivan, A. P.; Urbanski, S.; Yokelson, R. J.; Kreidenweis, S. M. Observations and analysis of organic aerosol evolution in some prescribed fire smoke plumes. *Atmos. Chem. Phys.* **2015**, *15* (11), 6323−6335.

(79) Donahue, N. M.; Epstein, S. A.; Pandis, S. N.; Robinson, A. L. A two-dimensional volatility basis set: 1. organic-aerosol mixing thermodynamics. *Atmos. Chem. Phys.* **2011**, *11* (7), 3303−3318.

(80) Donahue, N. M.; Kroll, J. H.; Pandis, S. N.; Robinson, A. L. A two-dimensional volatility basis set - Part 2: Diagnostics of organic-aerosol evolution. *Atmos. Chem. Phys.* **2012**, *12* (2), 615−634.